Analysis of Environmental Effect on Temperature Distribution of Power Converter for Switched Reluctance Motor Drive

H. Chen Y. Xu and Z. Hu
China University of Mining & Technology
Xuzhou, 21116, China
hchen@cumt.edu.cn

***Abstract*—This paper presents a coupled model of fluid-structure-thermal simulation of power converter for switched reluctance motor drive. The mathematical description is made up of mass conservation equations, momentum conservation equations and energy conservation equations. The accuracy of the model is verified by comparing experimental data with simulation results derived from finite-element method. Furthermore, the analysis in the distance between the radiator and the fan, the height of the enclosure, and the air velocity of the fan is studied with the proposed model.**

Index Terms—**Thermal conductivity, temperature, thermal analysis, power converter.**

I. Introduction

The most of the previous work on switched reluctance motor (SRM) drive are in optimization of motor made of novel iron core material [1], rotor position estimation [2], magnetic characteristics [3], motor optimal design [4], temperature rise analysis of motors [5], monitoring system for rotor eccentricity detection [6], thermal-electromagnetic analysis for driving cycles [7].

In this paper, a model of environmental effect on temperature rise of power converter for SRM drive is developed to calculate the temperature rise distribution by using finite-element method (FEM). Considering dry and moist air, different convective heat transfer coefficient, different inlet velocity, the temperature rise distribution of the power converter is simulated with the proposed model and is verified by the experimental data.

II. Structure of Power Converter

The three-phase asymmetrical half-bridge main circuit is adopted. The power devices in main circuit include 12 power MOSFETs and 6 fast recovery diodes. The model is divided into three layers from top to bottom, such as power electronic devices, thermal insulating silicone gasket and aluminum finned radiator. The main circuit is installed in a box, and other wires inside are omitted to simplify the model, which is shown in Fig 1.

III. Simulation Model

A. Mass Conservation Equation

$$\frac{\partial \rho}{\partial t}+\frac{\partial(\rho u)}{\partial x}+\frac{\partial(\rho v)}{\partial y}+\frac{\partial(\rho w)}{\partial z}=0 \tag{1}$$

$$\frac{\partial \rho}{\partial t}+div(\rho U)=0 \tag{2}$$

$$\frac{\partial(\rho u)}{\partial x}+\frac{\partial(\rho v)}{\partial y}+\frac{\partial(\rho w)}{\partial z}=0 \tag{3}$$

where, ρ is density, t is time, $\boldsymbol{U}$ is velocity vector, u, v and w are components of the velocity vector $\boldsymbol{U}$.

B. Momentum Conservation Equation

$$\frac{\partial(\rho u)}{\partial t}+div(\rho u U)=\frac{\partial p}{\partial x}+\frac{\partial \tau_{xx}}{\partial x}+\frac{\partial \tau_{yx}}{\partial y}+\frac{\partial \tau_{zx}}{\partial z}+F_x \tag{4}$$

$$\frac{\partial(\rho v)}{\partial t}+div(\rho v U)=\frac{\partial p}{\partial y}+\frac{\partial \tau_{xy}}{\partial x}+\frac{\partial \tau_{yy}}{\partial y}+\frac{\partial \tau_{zy}}{\partial z}+F_y \tag{5}$$

$$\frac{\partial(\rho w)}{\partial t}+div(\rho w U)=\frac{\partial p}{\partial z}+\frac{\partial \tau_{xz}}{\partial x}+\frac{\partial \tau_{yz}}{\partial y}+\frac{\partial \tau_{zz}}{\partial z}+F_z \tag{6}$$

where, p is the force; τ_{xx}, τ_{yx} and τ_{zx} are the components of the τ: F_x, F_y and F_z are the force on the Infinitesimal body.

C. Energy Conservation Equation

$$\frac{\partial(\rho T)}{\partial t}+div(\rho U T)=div\left(\frac{k}{c_p}\,grad T\right)+S_T \tag{7}$$

where, c_p is Specific heat capacity, T is temperature, k is the heat transfer coefficient, S_T is the heat source and the part of the mechanical energy changing into heat energy because of viscous effect.

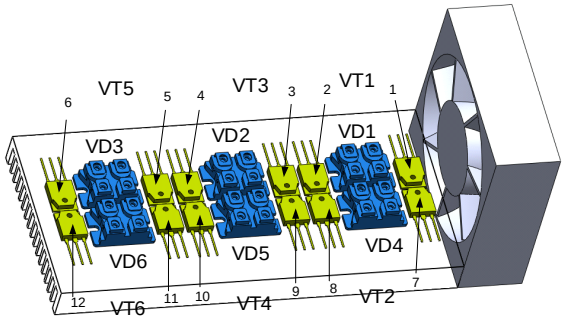

Fig. 1. Structure of power converter.

IV. Calculated Results and Experimental Validation

Fig. 2 shows the temperature contours of the power converter using a fan cooling. It is shown that the temperature of the power converter near the fan is lower than that of away from the fan. The two power MOSFETs on the left get the maximum temperature of 24.80°C. The temperature distribution of the power converter is vertically symmetric, so that it can be appropriately simplified for analysis.

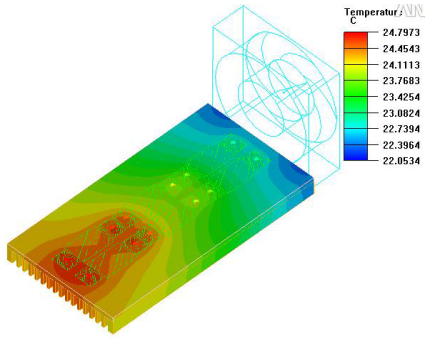

Fig. 2. Temperature contours distribution of power converter.

Fig. 3 shows the fluid velocity vector distribution in the central slice along the fin's direction, where the air volume of the fan is 118 cubic feet per minute. As shown in Fig. 3, due to the viscous effect, the fluid velocity near the enclosure becomes lower, which comes to 0m/s around the wall surface. In most of the space above the radiator, the fluid velocity is approximately the same as the inflow velocity. But the air velocity near the radiator especially the inlet velocity comes to 10m/s which exceeds the fan velocity since spatial decreasing increases the air velocity with meeting the law of mass conservation.

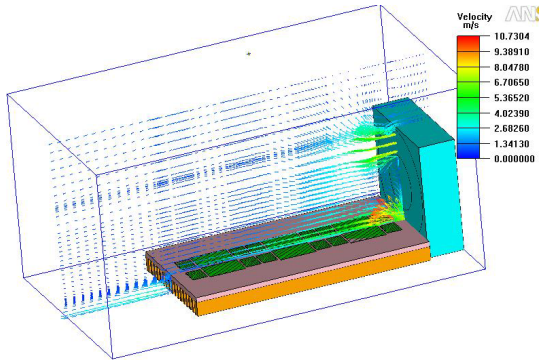

Fig. 3. Velocity vector distribution in the central slice along the fin's direction.

Fig. 4 shows the comparison of measured temperature rise and simulated results. The twelve test points are used to measure the central point temperature rise of the twelve power MOSFETs. It is shown that the simulated data agree well with the experimental results, showing the same trend and magnitude of change. The error range of the proposed in the test points is from -1.7^{0}C to 1.0^{0}C. Therefore, the proposed coupled model of fluid-structure-thermal simulation is adopted to predict the system temperature rise.

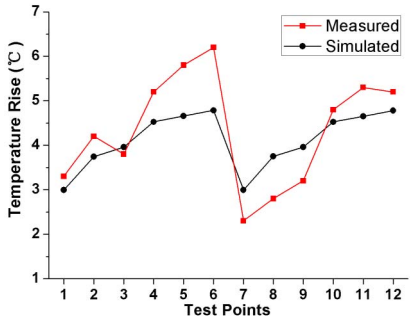

Fig. 4. Comparison of experimental results and simulated results.

V. Placement and Air Velocity

In order to enhance the heat transfer ability of power converter, the distance between the radiator and the fan, the height of the enclosure, and the air velocity of the fan, are studied by using the proposed model in this paper. The parameter symbols are illustrated in Fig. 5, while *L* is the distance between the radiator and the fan, *h* is the height of the enclosure.

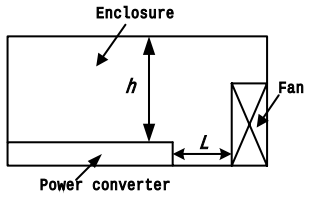

Fig. 5. Geometry size.

In order to study the influence of heat transfer ability, the distance of the radiator and the fan is changed from 0mm to 30mm with 5mm increased. It is shown that the simulated data agree well with the experimental results in the same trend. With the increase of the height, the temperature rise has a little increase, so that the height has little effect on the heat dissipation. In case of constant fluid flow volume, the increment of the height makes the velocity around the radiator decreased slightly, which leads to the tiny increase of the temperature rise on the power electronic components.

VI. Conclusion

In this paper, a coupled model of fluid-structure-thermal simulation for power converter in switched reluctance motor drive has been introduced. This model can predict the temperature rise distribution in power converter by compulsive ventilation cooling, study the distance between the radiator and the fan, the height of the enclosure, and the air velocity of the fan. The accuracy of the model is verified by comparing experimental data with those resulting derived from FEM simulation.

References

[1] Y. Hasegawa, K. Nakamura and O. Ichinokura, "Optimization of a switched reluctance motor made of permendur," *IEEE Trans. on Magnetics*, vol.46, no.6, pp.1311–1314, June 2010.

[2] K. Geldhof, P. Sergeant, A. V. D. Bossche and J. Melkebeek, "Analysis of hysteresis in resonance-based position estimation of switched reluctance drivesr," *IEEE Trans. on Magnetics*, vol.47, no.5, pp.1022-1025, May 2011.

[3] L. Bernard, X. Mininger, L. Daniel, G. Krebs, F. Bouillault and M. Gabsi, "Effect of stress on switched reluctance motors: a magneto-elastic finite-element approach based on multiscale constitutive laws," *IEEE Trans. on Magnetics*, vol.47, no.9, pp.2171-2179, Sept. 2011.

[4] A. Kechroud, J. J. H. Paulides and E. A. Lomonova, "B-spline neural network approach to inverse problems in switched reluctance motor optimal design," *IEEE Trans. on Magnetics*, vol.47, no.10, pp.4179-4182, Oct. 2011.

[5] J. Faiz, B. Ganji, C.E. Carstensen, K.A. Kasper and R.W. De Doncker, "Temperature rise analysis of switched reluctance motors due to electromagnetic losses," *IEEE Trans. on Magnetics*, vol.45, no.7, pp.2927-2934, July 2009.

[6] D.G. Dorrell and C. Cossar, "A vibration-based condition monitoring system for switched reluctance machine rotor eccentricity detection," *IEEE Trans. on Magnetics*, vol.44, no.9, pp.2204 - 2214, Sept. 2008.

[7] G. J. Li, J. Ojeda, E. Hoang, M. Lecrivain, and M. Gabsi, "Comparative studies between classical and mutually coupled switched reluctance motors using thermal-electromagnetic analysis for driving cycles," *IEEE Trans. on Magnetics*, vol.47, no.4, pp.839-861, April 2011.